Int. J. Electrochem. Sci., 10 **(2015)** 5961 - 5969

International Journal of
ELECTROCHEMICAL
SCIENCE
www.electrochemsci.org

Electrodeposition of ZnO-RGO thin film for determining Hg(II) in water samples

Yan Zhuang[*], *Jianhua Sun and Yunming Guan*

School of Chemistry & Chemical Engineering, Jiang Su University of Technology, ChangZhou City, Jiangsu P. R. China
[*]E-mail: yanzhuang2015@yahoo.com

Received: 27 March 2015 / *Accepted:* 22 April 2015 / *Published:* 27 May 2015

In this paper, we developed an electrochemical sensor for the detection of Hg^{2+} in various water samples. The electrochemical sensor was prepared by electrodeposition of ZnO nanostructures on an indium tin oxide (ITO). The ZnO thin film was then covered by a layer of graphene oxide (GO) using dip coating method. Subsequently, the GO layer was electrochemically reduced and forms ZnO-reduced graphene oxide (RGO). The obtained thin film was characterized by a series of techniques. Then, the electrochemical parameters of using proposed sensor for Hg(II) detection were optimized. Results indicated the sensor is suitable for Hg(II) detection in various water samples.

Keywords: ZnO; Reduced graphene oxide; Electrochemical sensor; Hg(II); Water samples

1. INTRODUCTION

Mercuric ion with highly physiological toxicity is a widespread pollutant, which can cause a number of health problems such as brain damage and kidney failure [1-4]. Even in low concentration, Hg^{2+} is a threat to the environment as well as human health due to its non-biodegradable and can enter food chain [5]. Moreover, water soluble divalent Hg^{2+} is one of the most usual and stable forms of mercury pollution [6]. Therefore, detection and monitoring of the Hg^{2+} level in various water system is an important issue for both the environment and human health. To date, many methods have been developed for the detection of Hg^{2+}, such as surface enhanced Raman spectroscopy [7], fluorescent method [8-10], atomic absorption spectrometry [11], inductively coupled plasma mass spectrometry [12], colorimetric sensor [13, 14], photoelectrochemical biosensor [15] and electrochemical sensor [16-30]. Among these approaches, due to the relatively high efficiency, cost-effectiveness, speed,

portability, ease of operation and reliability, electrochemical methods have become an important investigation domain for Hg^{2+} detection.

Different materials have been introduced into the electrochemical biosensor to improve its detection sensitivity. Zinc oxide (ZnO) is one of the well-studied transition metal oxide in electrochemistry. Some studies demonstrated that ZnO can be used for electrode surface modification and enhance its electrochemical activity. For example, Zhang et al. [31] reported the preparation of ultrathin ZnO nanofilms through a facile one-pot hydrothermal method. The prepared thin film was employed for determining glucose and hydrazine in solution. Tak et al. [32] reported the preparation of ZnO nanostructures based electrochemical DNA biosensor for bacterial meningitis detection. On the other hand, graphene has attracted a lot of attention due to its extremely high mobility thermal conductivity and strongly tunable electrical conduction [33, 34]. Therefore, it became a very hot material for in the field of electrochemistry. Many graphene modified electrodes have been reported due to their excellent electrochemical properties. For example, Yu and co-workers recently demonstrated the preparation of three-dimensional reduced graphene oxide and used for electrochemically determination of dopamine [35]. Rasheed and co-workers reported a graphene-DNA electrochemical sensor for the sensitive detection of BRCA1 gene [36].

Herein, we report the fabrication of a Hg^{2+} electrochemical sensor based on electrodeposited ZnO-electrochemically reduced graphene oxide (ZnO-RGO) hybrid thin film. The synthesized hybrid thin film was characterized by SEM, FTIR and XRD. The fabricated sensor was used for Hg^{2+} detection by cyclic voltammetry and differential pulse voltammetry. The results suggested that the ZnO-RGO modified ITO has a much higher current response and lower oxidation potential compared to its counterparts, bare ITO, ZnO and RGO modified ITO.

2. EXPERIMENTS

Synthetic graphite (average particle diameter <20 μm), $Hg(NO_3)_2$ and zinc nitrate hexahydrate ($Zn(NO_3)_2 \cdot 6H_2O$ were purchased from Sigma-Aldrich. All other chemicals used were analytical grade reagents without further purification. Milli-Q water (18.2 MΩ cm) was used throughout the experiments.

For electrodeposition of ZnO film. A platinum wire was used as the auxiliary electrode and an Ag/AgCl (3M KCl) as the reference electrode. The electrodeposition of ZnO film was performed using a ITO in 0.5 M HNO_3 solution containing 0.1 M $Zn(NO_3)$ using chronoamperometry at an applied potential of −0.9 V for 600s. The ZnO-RGO thin was fabricated in the following processes: graphene oxide (GO) was firstly prepared with the modified Hummers method with little modifications [37, 38]. The ZnO-GO thin film was fabricated by dip coating previously prepared ZnO thin film in 1 mg/mL GO dispersion. The electro-reduction of ZnO-GO to ZnO-RGO was conducted at 0.1 M pH 7.0 PBS solution with cyclic sweeping in the potential range from 0.0 to −1.4 V at a scan rate of 10 mV/s for 20 cycles. For DPV measurements, the accumulation time was 400 s, pulse amplitude was 50 mV, pulse width was 40 ms, scan rate was 40 mV/s.

The morphology of the thin films was characterized using a scanning electron microscope (SEM, S-4700, Hitachi High Technologies Corporation). The surface functional groups present on the samples were analyzed by Fourier transform infrared spectroscopy (FTIR, Nicolet iS5, Thermo Scientific, USA). The crystal phase information of sample was characterized from 5° to 80° in 2θ by a XRD with Cu Kα (λ = 0.1546 nm) radiation (D8-Advanced, Bruker).

3. RESULTS AND DISCUSSION

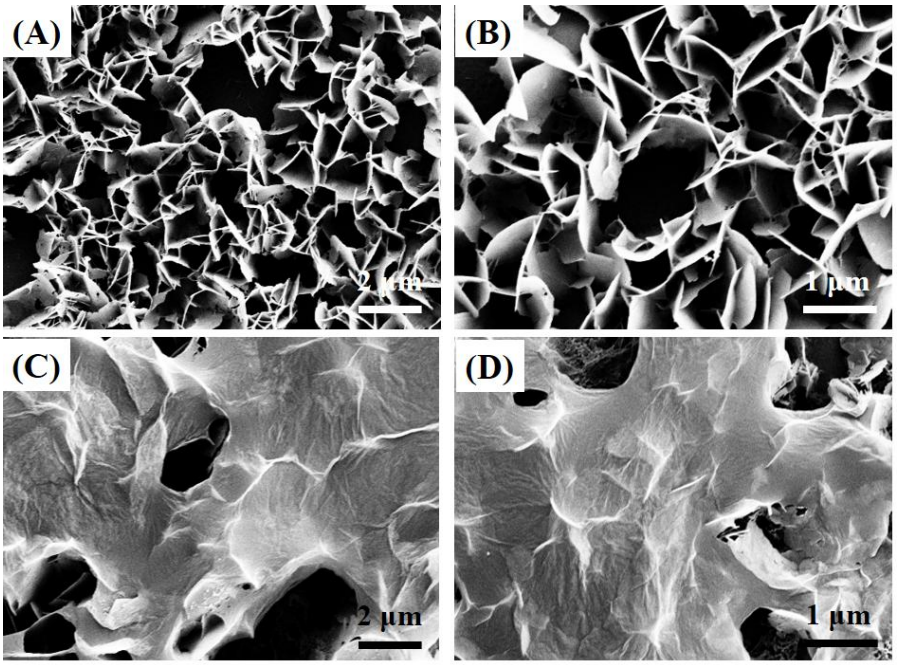

Figure 1. SEM images of (A, B) ZnO thin film and (C, D) ZnO-RGO thin film.

The morphology of the prepared thin films was characterized by SEM. Figure 1 shows the SEM images of ZnO and ZnO-RGO thin films at different magnifications. It can be observed that the electrodeposited ZnO thin film exhibits a porous structure, which consists of many nanoplates with approximate thickness of 30 nm (Figure 1A-B). This porous network structure with thin layer vertically arrayed ZnO nanoplate could provide a large specific surface area, which is favorable for the electrochemical reaction. After electro-reduction of GO, thin layer of RGO sheets were clearly deposited on the thin film surface, which could act as an electrical network between the ZnO nanoplates to improve the electrical conductivity of the thin film. Therefore, the proposed ZnO-RGO thin film could serve as an excellent candidate for electrochemical determination.

The XRD patterns of natural graphite powder, GO and ZnO and ZnO-RGO are presented in Figure 2A. It can be seen that the natural graphite powder exhibits a strong (002) peak at 26.49°, which indicates a typical pattern of crystal graphitic structure. The pristine GO displays a typical characteristic (001) peak at 11.1° [39]. For the electrodeposited ZnO, the peaks at 32.1°, 34.4°, 36.1°, 47.7°, 56.3°, 62.5° and 68.0° can be indexed to hexagonal ZnO (JCPDS 36-1451). After deposition of

GO film and subsequently electro-reduction process, the ZnO-RGO displays a similar XRD pattern compared with ZnO. It is worth noting that the GO peak completely disappeared in the hybrid sample, suggesting the RGO has been formed. Furthermore, the week peak at 24.08° in ZnO-RGO hybrid illustrates the exfoliated RGO incorporated with ZnO [40].

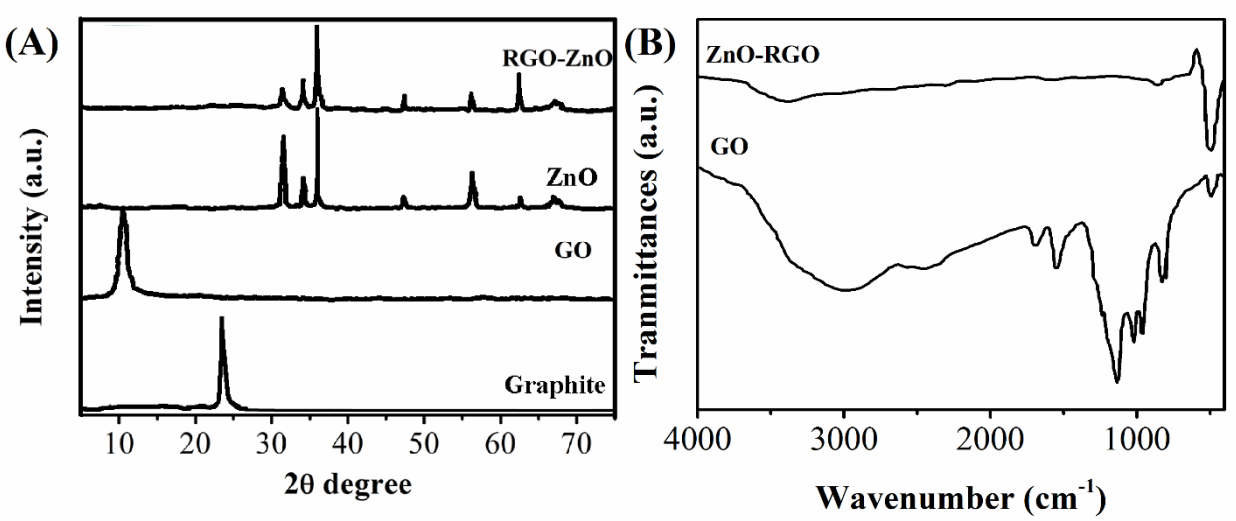

Figure 2. (A) XRD spectra of graphite, GO, ZnO and RGO-ZnO. (B) FTIR spectra of GO and ZnO-RGO.

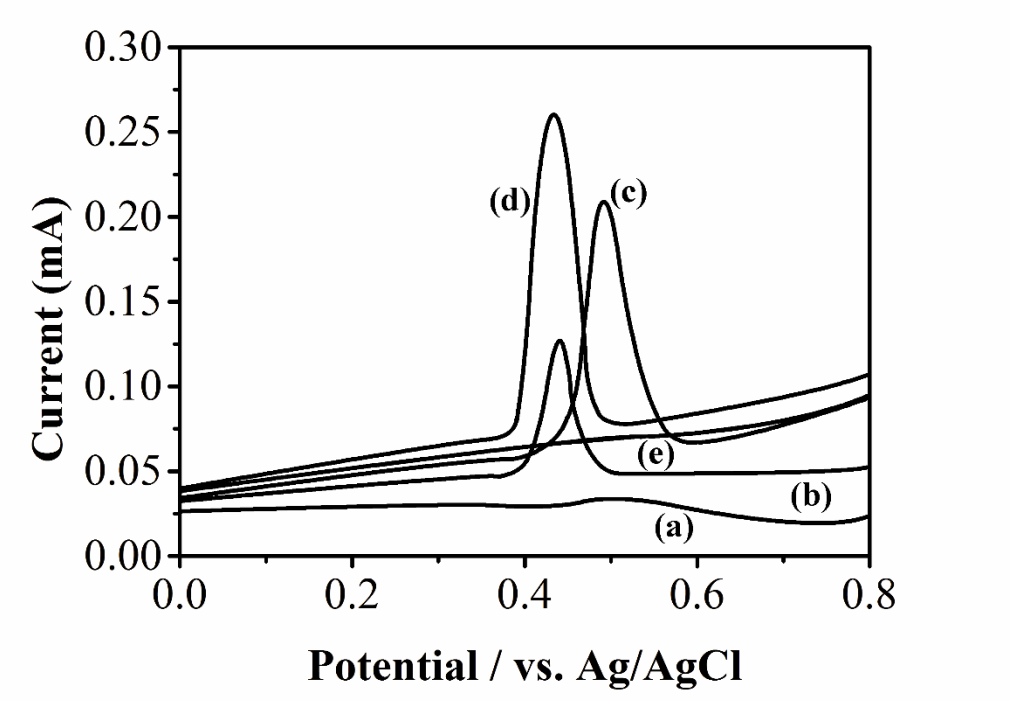

Figure 3. DPV of 0.5 μM Hg^{2+} recorded at (a) bare ITO, (b) RGO/ITO, (c) ZnO/ITO and (d) ZnO-RGO/ITO in 0.1 M HCl. (e) DPV of ZnO-RGO/ITO in 0.1 M HCl without Hg^{2+}.

The electro-reduction process and bonding interactions between ZnO and RGO was investigated by FTIR study. Figure 2B shows the FTIR spectra of GO and ZnO-RGO. The spectrum of GO shows peaks at 2940 cm^{-1}, 1729 cm^{-1}, 1401 cm^{-1} and 1052 cm^{-1}, which belong to the stretching vibration of CH_2, C═O stretching of COOH groups, C─OH stretching vibrations and C─O vibrations from alkoxy groups, respectively [41, 42]. The broad peak at 3342 cm^{-1} is assigned to the OH stretching vibration of oxygen functional groups. In addition, the peak at 1619 cm^{-1} is due to the sp^2 bond of graphite in GO [43]. Comparing spectra of ZnO-RGO with the GO, it is noticeable that the peaks related to oxygen functional groups are almost removed in GO by electro-reduction process, indicating the GO has been reduced considerably.[44] Moreover, there is an absorption peak at around 570 cm^{-1} can be observed in the spectrum of ZnO-RGO, corresponds to the stretching vibration of Zn─O bond [45].

Figure 3 shows the DPV response of different electrodes towards oxidation of 0.5 μM Hg^{2+} in the potential range of 0─0.8 V. At bare GCE, a small oxidation peak is observed at the potential of 0.53 V. While at RGO/ITO, an oxidation peak with peak current about 0.12 mA is observed at 0.43 V. The enhanced peak current and the negatively shifted oxidation potential can be ascribed to the excellent conductivity and electrocatalytic property of the RGO. In terms of ZnO/ITO, an even higher current response is observed at 0.52 V, indicating the electrodeposited ZnO thin film could highly facilitate the electron transfer on the electrode surface. On the other hand, the ZnO-RGO/ITO shows an oxidation peak at 0.43 V with peak current about 0.26 mA, which is approximately 12.5 times for bare ITO, 2.17 times for RGO/ITO and 1.3 times for ZnO/ITO. The enhancement of current response and lower the overpotential of Hg^{2+} oxidation in ZnO-RGO/ITO could ascribe to the high specific surface area, the excellent electrocatalytic property and the synergistic effect between ZnO and RGO.

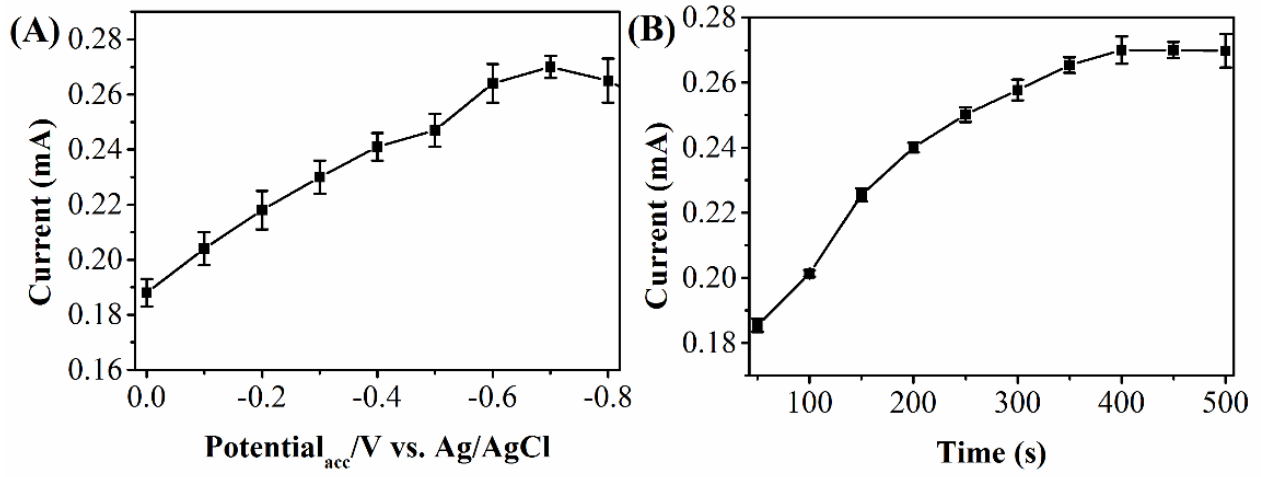

Figure 4. Effect of the (A) accumulation potential and (B) accumulation time on the current response of 0.5 μM Hg^{2+} at ZnO-RGO/ITO.

In order to enhance the electrochemical response, the accumulation step was adopted in this work. Figure 4 shows the effect of accumulation potential and time in the Hg^{2+} detection. As shown in

Figure 4A, the current response increases gradually from 0 to ─0.70 V and then slightly decreases when further increasing accumulation potential. On the other hand, the peak current increases gradually with the increase of accumulation time from 50 to 400 s and remains a similar performance if a longer accumulation time is applied (Figure 4B). Thus, the accumulation conditions of ─0.70 V and 400 s were adopted in further measurements.

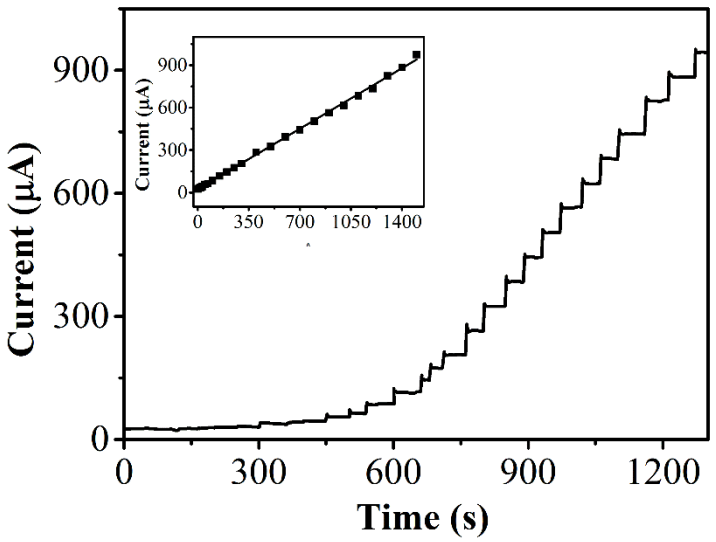

Figure 5. Amperometric response of the ZnO-RGO/ITO for the successive addition of Hg^{2+}. Applied potential: 0.43 V. Inset: The calibration curve for Hg^{2+} detection using ZnO-RGO/ITO.

The response time, linear range and detection limit of the ZnO-RGO/ITO for Hg^{2+} detection was then investigated. Figure 5 shows the typical amperometric responses of ZnO-RGO/ITO towards the successive addition of Hg^{2+} at a working potential of 0.43 V. It can be clearly observed that the current increases rapidly after the addition of Hg^{2+} and then returned to the steady-state within 2 s. This quick response time can be ascribed to the excellent electrocatalytic property and conductivity of ZnO-RGO hybrid. The amperometric response current increased linearly with Hg^{2+} concentrations between 0.001 μM and 1.5 μM, evident from the calibration plot (Inset Figure 5). The linear regression equation can be expressed as: I_{pa} (μA) = 0.61127 c (nM) + 23.1513 (R^2 = 0.998). The detection limit for Hg^{2+} is calculated to be 0.7 nM. The limit of detection has been calculated using the formula, limit of detection = 3 s_b/S where, s_b is the standard deviation of ten blank measurements and S is the sensitivity [46].

The interference study was investigated at the ZnO-RGO/ITO in the presence of other ions commonly present in drinking water. Under optimized experimental conditions, the DPV results indicated that the 50-folds of Cd^{2+}, Cr^{3+}, Zn^{2+}, Na^{+}, K^{+}, Pd^{2+}, Co^{2+}, Cl^{-} and I^{-} did not interfere with the analysis of Hg^{2+} (peak current changes are less than ±6%), indicating the high selectivity of the ZnO-RGO/ITO towards the determination of Hg^{2+}. The RSD for ten successive Hg^{2+} detection was 4.3% and five independent ZnO-RGO/ITO had an RSD of 4.1% for the determination of 0.5 μM Hg^{2+}, suggesting the excellent repeatability and reproducibility of the ZnO-RGO/ITO.

We further studied the feasibility of the ZnO-RGO/ITO for environmental and drinking water analysis. Tap water, rain water, bottle water and lake water were collected for analysis. The standard addition method was applied and the results were listed in Table 1.

Table 1. Determination of Hg^{2+} in water samples using ZnO-RGO/ITO.

Sample	Added (nM)	Found (nM)	Recovery (%)	RSD (%)
Tap water 1	0	0	—	0.25
Tap water 2	20	19.02	95.1	1.31
Rain water 1	50	51.20	102.4	2.02
Rain water 2	100	102.30	102.3	2.11
Bottle water 1	200	198.44	99.22	2.66
Bottle water 2	500	499.52	100.6	1.54
Lake water 1	500	504.21	99.9	3.55
Lake water 2	1000	1004.78	100.48	2.01

The results indicate that the recovery for the determination of Hg^{2+} was in the range of 95.1–102.4%, revealing that the ZnO-RGO/ITO could be used for accurate and feasible determining Hg^{2+} in various water samples.

4. CONCLUSION

A highly sensitive and selective electrochemical Hg^{2+} sensor was fabricated by electrodeposition of ZnO nanoplates on ITO surface followed by electro-reduction of GO thin film. FTIR analysis confirmed the formation of RGO during the electro-reduction process. The prepared ZnO-RGO/ITO was then used for determination of Hg^{2+}. The ZnO-RGO/ITO showed a linear response in the Hg^{2+} range between 0.001 to 1.5 μM. The observed limit of detection is well below the World Health Organization guideline value for Hg^{2+} in drinking water. Therefore, the proposed ZnO-RGO/ITO is a suitable electrode material for the determination of Hg^{2+}in water samples.

ACKNOWLEDGEMENTS
The authors gratefully thank the Financial 423 supports from the National Natural Science Foundation of China 424 (Contract Number: 21373103) and Jiangsu Province Natural Science 425 Foundation (No. BK2011260).

Reference

1. M. Harada, *Critical Reviews in Toxicology*, 25 (1995) 1
2. H.N. Kim, M.H. Lee, H.J. Kim, J.S. KimandJ. Yoon, *Chemical Society Reviews*, 37 (2008) 1465
3. V.M. Galimova, I.V. Surovtsev, V.V. Mank, V.A. KopilevichandV.I. Maksin, *J. Water Chem. Technol.*, 35 (2013) 210

4. L. Fu, Y. Zheng, A. Wang, W. CaiandH. Lin, *Food Chemistry*, 181 (2015) 127
5. Q.H. Zhang, L. Huang, Y. Zhang, C.H. KeandH.Q. Huang, *Journal of Proteomics*, 94 (2013) 37
6. E. Akkemik, P. Taser, A. Bayindir, H. BudakandM. Ciftci, *Environmental Toxicology and Pharmacology*, 34 (2012) 888
7. M. Liu, Z. Wang, S. Zong, H. Chen, D. Zhu, L. Wu, G. HuandY. Cui, *ACS applied materials & interfaces*, 6 (2014) 7371
8. Z.-X. WangandS.-N. Ding, *Analytical Chemistry*, 86 (2014) 7436
9. L. Fu, A. Wang, Y. Zheng, W. CaiandZ. Fu, *Materials Letters*, 142 (2015) 119
10. Y. Zheng, A. Wang, H. Lin, L. FuandW. Cai, *RSC Advances*, 5 (2015) 15425
11. T. LabatzkeandG. Schlemmer, *Anal Bioanal Chem*, 378 (2004) 1075
12. M. Wang, W. Feng, J. Shi, F. Zhang, B. Wang, M. Zhu, B. Li, Y. ZhaoandZ. Chai, *Talanta*, 71 (2007) 2034
13. Z. Mohammadpour, A. SafaviandM. Shamsipur, *Chemical Engineering Journal*, 255 (2014) 1
14. L. Fu, Y. Zheng, Z. Wang, A. Wang, B. DengandF. Peng, *Digest Journal of Nanomaterials and Biostructures*, 10 (2015) 117
15. Z.-Y. Ma, J.-B. Pan, C.-Y. Lu, W.-W. Zhao, J.-J. XuandH.-Y. Chen, *Chemical Communications*, 50 (2014) 12088
16. Y. Wei, R. Yang, J.-H. LiuandX.-J. Huang, *Electrochimica Acta*, 105 (2013) 218
17. N. Zhou, J. Li, H. Chen, C. LiaoandL. Chen, *The Analyst*, 138 (2013) 1091
18. S. Palanisamy, R. Madhu, S.-M. ChenandS.K. Ramaraj, *Analytical Methods*, 6 (2014) 8368
19. Z. Wu, L. Jiang, Y. Zhu, C. Xu, Y. YeandX. Wang, *Journal of Solid State Electrochemistry*, 16 (2012) 3171
20. X. Lu, X. Dong, K. ZhangandY. Zhang, *Analytical Methods*, 4 (2012) 3326
21. D. Li, J. Li, X. JiaandE. Wang, *Electrochemistry Communications*, 42 (2014) 30
22. A. Dago, C. Ariño, J.M. Díaz-CruzandM. Esteban, *International Journal of Environmental Analytical Chemistry*, 94 (2014) 668
23. M. Wang, W. Yuan, X. YuandG. Shi, *Anal Bioanal Chem*, 406 (2014) 6953
24. G. Sai-Anand, A.-I. Gopalan, S.-W. Kang, S. KomathiandK.-P. Lee, *Science of Advanced Materials*, 6 (2014) 1356
25. A. Wang, H.P. Ng, Y. Xu, Y. Li, Y. Zheng, J. Yu, F. Han, F. PengandL. Fu, *Journal of Nanomaterials*, 2014 (2014) 6
26. L. FuandZ. Fu, *Ceram Int*, 41 (2015) 2492
27. L. Fu, Y. Zheng, A. Wang, W. Cai, Z. FuandF. Peng, *Sensor Letters*, 13 (2015) 81
28. L. Fu, Y. Zheng, Q. Ren, A. WangandB. Deng, *Journal of Ovonic Research*, 11 (2015) 21
29. L. Fu, T. Xia, Y. Zheng, J. Yang, A. WangandZ. Wang, *Ceram Int*, 41 (2015) 5903
30. L. Fu, W. Cai, A. WangandY. Zheng, *Materials Letters*, 142 (2015) 201
31. X. Zhang, W. Ma, H. NanandG. Wang, *Electrochimica Acta*, 144 (2014) 186
32. M. Tak, V. GuptaandM. Tomar, *Biosensors and Bioelectronics*, 59 (2014) 200
33. A.A. Balandin, *Nat Mater*, 10 (2011) 569
34. A.K. GeimandK.S. Novoselov, *Nat Mater*, 6 (2007) 183
35. B. Yu, D. Kuang, S. Liu, C. LiuandT. Zhang, *Sensors and Actuators B: Chemical*, 205 (2014) 120
36. P.A. RasheedandN. Sandhyarani, *Sensors and Actuators B: Chemical*, 204 (2014) 777
37. W.S. HummersandR.E. Offeman, *Journal of the American Chemical Society*, 80 (1958) 1339
38. T. GanandS. Hu, *Microchim Acta*, 175 (2011) 1
39. T. Nakajima, A. MabuchiandR. Hagiwara, *Carbon*, 26 (1988) 357
40. C. Xu, X. WangandJ. Zhu, *J Phys Chem C*, 112 (2008) 19841
41. C. NethravathiandM. Rajamathi, *Carbon*, 46 (2008) 1994
42. M. Ahmad, E. Ahmed, Z.L. Hong, J.F. Xu, N.R. Khalid, A. ElhissiandW. Ahmed, *Appl Surf Sci*, 274 (2013) 273
43. X. Li, Q. Wang, Y. Zhao, W. Wu, J. ChenandH. Meng, *Journal of colloid and interface science*,

411 (2013) 69
44. D. BoukhvalovandM. Katsnelson, *Physical Review B*, 78 (2008) 085413
45. Q.-P. Luo, X.-Y. Yu, B.-X. Lei, H.-Y. Chen, D.-B. KuangandC.-Y. Su, *J Phys Chem C*, 116 (2012) 8111
46. V. Mani, B. DevadasandS.-M. Chen, *Biosensors and Bioelectronics*, 41 (2013) 309